Int. J. Electrochem. Sci., 17 **(2022)** Article Number: 220831, doi: 10.20964/2022.08.21

International Journal of
ELECTROCHEMICAL
SCIENCE
www.electrochemsci.org

Influence of Synergistic Effect of Hydroxylamine Sulphate and Ultrasonic Vibration on Corrosion Resistance of Zinc Phosphating Coating Prepared on 20# Steel

Lin Hongli[1,*], *Song Chao*[2], *Yi Shuli*[1], *Yu Qun*[1]

[1] Qingdao Huanghai University, Qingdao 266427, China;
[2] Zhejiang Jiangnan Engineering Management Limited Company, Hangzhou 310000, China
[*]E-mail: Lin_edu266@126.com

Received: 6 May 2022 / *Accepted:* 1 June 2022 / *Published:* 4 July 2022

Hydroxylamine sulphate was added to the phosphating solution and constant-intensity ultrasonic vibration was applied during the zinc phosphating treatment of 20# steel. The influence of synergistic effect of hydroxylamine sulphate and constant-intensity ultrasonic vibration on the appearance, surface morphology, phase and corrosion resistance of zinc phosphating coating was studied, and was compared with hydroxylamine sulphate or constant-intensity ultrasonic vibration alone. The results show that the zinc phosphating coating is incomplete without hydroxylamine sulphate and has poor corrosion resistance. Both hydroxylamine sulphate and constant-intensity ultrasonic vibration contribute to the formation of a complete and relatively dense zinc phosphating coating, which is primarily composed of $Zn_3(PO_4)_2{\cdot}4H_2O$ and $Zn_2Fe(PO_4)_2{\cdot}4H_2O$ phases with better corrosion resistance. The synergistic effect of hydroxylamine sulphate and constant-intensity ultrasonic vibration can not only reduce the added amount of hydroxylamine sulphate but likewise prepare a zinc phosphating coating with better compactness and optimal corrosion resistance, which can better inhibit the corrosion of 20# steel.

Keywords: Zinc phosphating coating; Corrosion resistance; Hydroxylamine sulphate; Constant-intensity ultrasonic vibration; Synergistic effect

1. INTRODUCTION

Traditional chemical conversion coating is a commonly utilised surface treatment process for steel components prior to painting, such as phosphating coating, passivation coating, and so on [1-6]. Phosphating coating, in particular, has the advantages of simple operation and low cost, and has received widespread attention. Hydroxylamine sulphate is an employed accelerant in phosphating process. Compared with the toxic oxidizing accelerants such as sodium nitrate, sodium nitrite and

potassium chlorate, hydroxylamine sulphate offers non-toxicity, and environmental protection, along with better stability [7]. However, the consumption rate of hydroxylamine sulphate during phosphating process is fast. In order to ensure the quality and performance of the phosphating coating, hydroxylamine sulphate must be added frequently, making the phosphating solution difficult to stabilise. Therefore, to ensure the quality and performance of the phosphating coating, reducing the added amount and adding times of hydroxylamine sulphate is necessary.

Some scholars have proposed the idea of mixing the hydroxylamine sulphate with other accelerants for phosphating solution, such as the mixing of hydroxylamine sulphate and sodium chlorate, the mixing of hydroxylamine sulphate and sodium nitrobenzenesulfonate, and so on [8-11]. Even though the amount of hydroxylamine sulphate added can be lowered, the introduction of other reagents is also not conducive to the maintenance of phosphating solution. Some studies have confirmed that introducing ultrasonic vibration in the chemical reaction process can accelerate the chemical reaction rate [12-16]. In the phosphating process, if hydroxylamine sulphate and ultrasonic vibration are used synergistically, it can not only reduce the added amount of hydroxylamine sulphate, but also is expected to obtain a phosphating coating with good quality and performance. In this paper, different zinc phosphating coatings are prepared on the surface of 20# steel. During the phosphating process, hydroxylamine sulphate is added as an accelerant and constant-intensity ultrasonic vibration is introduced so as to improve the morphology and corrosion resistance of the zinc phosphating coating. The research conclusions have reference value for optimizing the zinc phosphating process.

2. EXPERIMENTAL

2.1 Pretreatment of 20# steel substrate

The chemical composition of 20# steel plate is 0.14~0.22% C, 0.30~0.65% Mn, 0.30% Si, 0.05% P, 0.05% S, and the rest is Fe. The 20# steel plate was cut into 40 mm×20 mm×2 mm as the substrate. And then, the substrate was polished, degreased, activated, cleaned and dried sequentially before the experiment.

2.2 Preparation of zinc phosphating coating

An electronic balance was used to weigh analytical pure reagents such as zinc dihydrogen phosphate 40 g/L, zinc nitrate 80 g/L, phosphoric acid 12 g/L and citric acid 2 g/L, which was dissolved and stirred evenly. And then distilled water was added to prepare 1200 mL basic zinc phosphating solution. The basic zinc phosphating solution was divide into four equal portions of 300 mL each and put in labeled beakers A, B, C and D. Beakers A and B were placed in an ordinary water solution at the temperature of (50±0.5)℃. Beakers C and D were placed in a water solution equipped with an ultrasonic generator and the temperature was also controlled at (50±0.5)℃. The ultrasonic power and ultrasonic frequency were set to 135 W and 40 kHz respectively, and the constant-intensity ultrasonic vibration was transmitted to the phosphating solution through water as the medium. The

constant-intensity ultrasonic vibration applied to the phosphating solution produces a special effect, which affects the crystallization process of phosphate precipitation and changes the performance of zinc phosphating coating. Hydroxylamine sulphate was used as accelerant and added to beakers B and D at a concentration of 3 g/L and 1.8 g/L, respectively.

The pretreated substrates were immersed in beakers A, B, C and D for 16 min respectively, and a series of reactions occurred on the surface of the substrate to generate four kinds of zinc phosphating coatings. After the experiment, the samples were cleaned and dried.

2.3 Testing of zinc phosphating coatings

2.3.1 Surface morphology characterization and composition analysis

The surface morphology and composition of different zinc phosphating coatings were characterized by VEGA II XMU scanning electron microscope combined with X-Max 50 energy dispersive spectrometer. The magnification of scanning electron microscope was 1000 times. The working mode of energy dispersive spectrometer was set as surface scanning.

2.3.2 Phase analysis

D8 Advance X-ray diffraction and Jade software were used to analyze the phase of different zinc phosphating coatings. The scanning step length was 0.02° and the scanning angle was ranged from 15° to 85°.

2.3.3 Corrosion resistance testing

The polarization curves and electrochemical impedance spectroscopy of different zinc phosphating coatings immersed in 3.5% sodium chloride solution for 96 h were tested using a CHI660E type electrochemical workstation. The three-electrode system was as follows: phosphated samples were utilised as the working electrode with 10 mm×10 mm exposed working area while the platinum was employed as the auxiliary electrode and saturated calomel electrode was used as the reference electrode. The scanning rate of polarization curve was 1 mV/s, and the scanning potential ranged from -250 mV to +250 mV. The frequency range of electrochemical impedance spectroscopy was 100 kHz~10 mHz, and the signal amplitude was 10 mV.

Moreover, the corrosion morphology of different phosphating coatings immersed in 3.5% sodium chloride solution for 96 h was characterized by scanning electron microscopy. The corrosion products on the surface were removed and the corrosion weight loss of different zinc phosphating coatings were calculated by weighing.

3. RESULTS AND DISCUSSION

3.1 Appearance of different zinc phosphating coatings

During the experiment, it is observed that the zinc phosphating coating is incomplete without hydroxylamine sulphate, as shown in Figure 1(b). However, a complete and compact zinc phosphating coating with compact gray appearance can be prepared by adding hydroxylamine sulphate, as shown in Figure 1(c). This is because hydroxylamine sulphate aids in promoting phosphating reaction and accelerating phosphate precipitation crystallization in order to form a compact phosphating coating. The function of hydroxylamine sulphate or hydroxylamine is studied in some papers [17-18]. A compact phosphating coating can also be prepared by introducing constant-intensity ultrasonic vibration, as shown in Figure 1(d). Due to the cavitation effect caused by constant-intensity ultrasonic vibration transmission in phosphating solution, the local high-temperature effect and micro jet effect promote the chemical reaction and accelerate the formation of a zinc phosphating coating with compact surface [19-20]. Moreover, the appearance and compactness of zinc phosphating coating prepared by synergistic effect of hydroxylamine sulphate and constant-intensity ultrasonic vibration are nearly identical to those prepared by hydroxylamine sulphate or constant-intensity ultrasonic vibration alone, as shown in Figure 1(e).

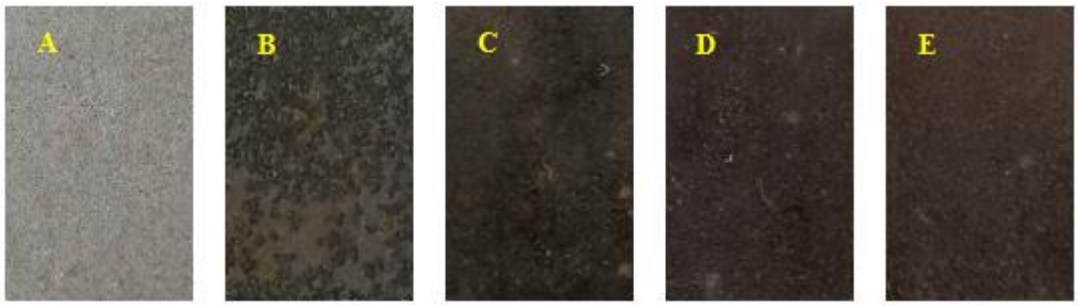

Figure 1. Appearance of 20# steel and different zinc phosphating coatings: A-20# steel; B-zinc phosphating coating (without hydroxylamine sulphate and constant-intensity ultrasonic vibration); C-zinc phosphating coating (adding hydroxylamine sulphate); D-zinc phosphating coating (introducing constant-intensity ultrasonic vibration); E-zinc phosphating coating (synergistic effect of hydroxylamine sulphate and constant-intensity ultrasonic vibration)

3.2 Surface morphology of different zinc phosphating coatings

Figure 2(a) shows the surface morphology of 20# steel and Figure 2(b) shows the surface morphology of zinc phosphating coating prepared without hydroxylamine sulphate. By comparison, the zinc phosphating coating prepared without hydroxylamine sulphate is thin and incomplete, and the surface of 20# steel is not completely covered. Figure 2(c)~2(e) shows the surface morphology of zinc phosphating coating prepared by adding hydroxylamine sulphate, introducing constant-intensity ultrasonic vibration and synergistic effect of hydroxylamine sulphate and constant-intensity ultrasonic vibration respectively. As can be seen from Figure 2(c), the zinc phosphating coating prepared by

adding hydroxylamine sulphate is complete and compact on the surface of 20# steel, and the grains have a flake shape with disordered accumulation. Because hydroxylamine sulphate is a reductive accelerant, its high reduction potential can play a depolarization role in the phosphating process for the purpose of eliminating hydrogen ions on the surface of the cathode region, which is conducive to improving the phosphating coating forming efficiency. At the same time, it also has a strong oxidation ability and stimulates the phosphating reaction so as to accelerate phosphate precipitation crystallization to form phosphating coating. As can be seen from Figure 2(d), the zinc phosphating coating prepared by introducing constant-intensity ultrasonic vibration also completely covers the surface of 20# steel, but the grains are staggered and stacked in lamellar and rod-like structure, which is different from the zinc phosphating coating prepared by adding hydroxyamine sulphate. It can be concluded that cavitation effect induced by transmission of constant-intensity ultrasonic vibration in phosphating solution produces a powerful shock wave that refines parts of the primary grain and causes grain morphology to change. Compared with Figure 2(c), the compactness of the zinc phosphating coating shown in Figure 2(d) has been improved. As reported in the literature, the grains refined by ultrasonic vibration cavitation effect are dispersed and can minimise the crystallization defects, thereby improving the compactness of zinc phosphating coating to some extent [21-22].

It can be seen from Figure 2(e) that the synergistic effect of hydroxylamine sulphate and constant-intensity ultrasonic vibration can prepare a zinc phosphating coating with better compactness under the condition of reducing the added amount of hydroxylamine sulphate. The synergistic mechanism of hydroxylamine sulphate and constant-intensity ultrasonic vibration can be summarized into two aspects: on the one hand, the cavitation effect caused by the transmission of constant-intensity ultrasonic vibration in the phosphating solution promotes the full dispersion of hydroxylamine sulphate, drives the hydrolysis of zinc dihydrogen phosphate, while also accelerating the phosphate precipitation on the surface of 20# steel. The cavitation effect caused by ultrasonic vibration has been proved and reported by some scholars in detail [23-25]. Simultaneously, the local high temperature causes the coating formation period to be shortened and the nucleation rate to be increased, resulting in more compact phosphating coating. On the other hand, the transmission of constant-intensity ultrasonic vibration in the phosphating solution produces a strong shock wave, which can produce many small heterogeneous crystal nuclei. The phosphating coating formation with compact surface morphology can be promoted by the adsorption of hydroxylamine sulphate on the surface of these crystal nuclei.

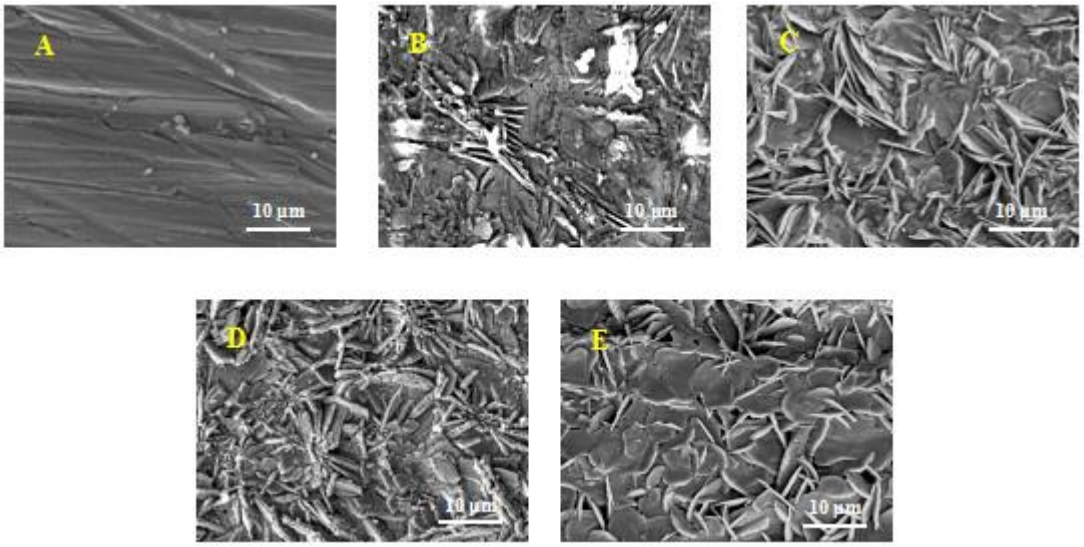

Figure 2. Surface morphology of 20# steel and different zinc phosphating coatings: A-20# steel; B-zinc phosphating coating (without hydroxylamine sulphate and constant-intensity ultrasonic vibration); C-zinc phosphating coating (adding hydroxylamine sulphate); D-zinc phosphating coating (introducing constant-intensity ultrasonic vibration); E-zinc phosphating coating (synergistic effect of hydroxylamine sulphate and constant-intensity ultrasonic vibration)

3.3 Phase and surface composition of different zinc phosphating coatings

The zinc phosphating coating prepared without hydroxylamine sulphate is incomplete, so structure analysis is not performed. Figure 3 shows the XRD patterns of zinc phosphating coating prepared by adding hydroxylamine sulphate, introducing constant-intensity ultrasonic vibration and synergistic effect of hydroxylamine sulphate and constant-intensity ultrasonic vibration respectively. The comparison shows that adding hydroxylamine sulphate, introducing constant-intensity ultrasonic vibration and synergistic effect of hydroxylamine sulphate and constant-intensity ultrasonic vibration have little effect on the structure of zinc phosphating coating. All the zinc phosphating coatings are composed of $Zn_3(PO_4)_2{\cdot}4H_2O$ and $Zn_2Fe(PO_4)_2{\cdot}4H_2O$ phases.

Figure 4 shows the surface composition of different zinc phosphating coatings prepared by adding hydroxylamine sulphate, introducing constant-intensity ultrasonic vibration and synergistic effect of hydroxylamine sulphate and constant-intensity ultrasonic vibration respectively. Zn, O, P and Fe elements are detected on the surface of different zinc phosphating coatings with little difference in the mass fraction of each element. These elements are important elements for the formation of $Zn_3(PO_4)_2{\cdot}4H_2O$ and $Zn_2Fe(PO_4)_2{\cdot}4H_2O$ phases. The similar composition and structure of zinc phosphating coating can also be found in some paper [26-27].

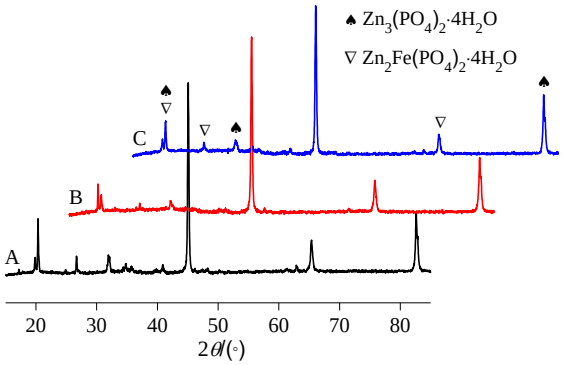

Figure 3. XRD patterns of different zinc phosphating coatings: A-zinc phosphating coating (adding hydroxylamine sulphate); B-zinc phosphating coating (introducing constant-intensity ultrasonic vibration); C-zinc phosphating coating (synergistic effect of hydroxylamine sulphate and constant-intensity ultrasonic vibration)

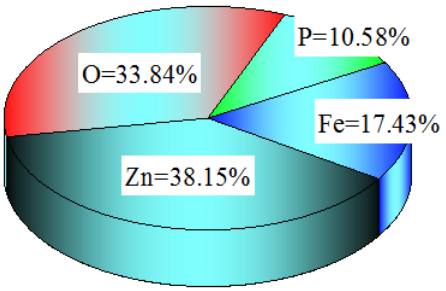

A-zinc phosphating coating (adding hydroxylamine sulphate)

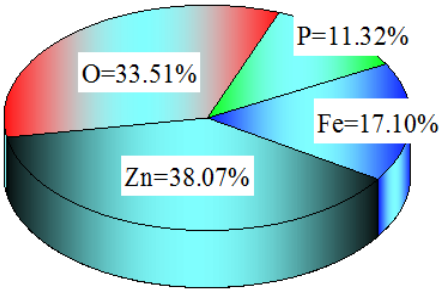

B-zinc phosphating coating (introducing constant-intensity ultrasonic vibration)

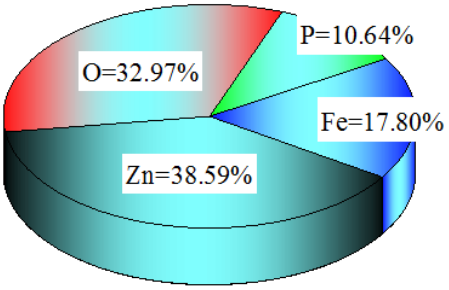

C-zinc phosphating coating (synergistic effect of hydroxylamine sulphate and constant-intensity ultrasonic vibration)

Figure 4. Surface composition of different zinc phosphating coatings

3.4 Corrosion resistance of different zinc phosphating coatings

3.4.1 Polarization curves analysis

Figure 5 shows the polarization curves of 20# steel and different zinc phosphating coatings immersed in 3.5% sodium chloride solution for 96 h. As can be seen from Figure 5, the polarization curve of the zinc phosphating coating prepared without hydroxylamine sulphate does not deviate significantly from that of 20# steel, indicating that the zinc phosphating coating could not effectively inhibit corrosion of 20# steel.

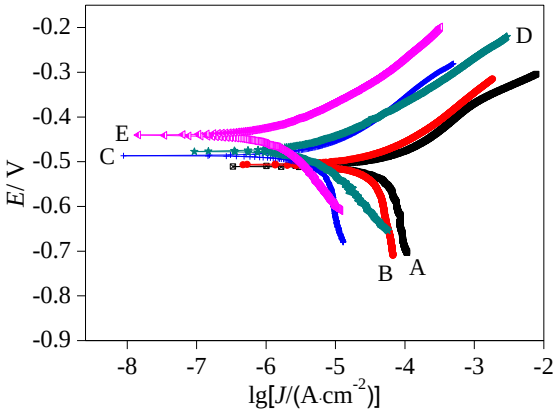

Figure 5. Polarization curves of 20# steel and different zinc phosphating coatings immersed in 3.5% sodium chloride solution for 96 h: A-20# steel; B-zinc phosphating coating (without hydroxylamine sulphate and constant-intensity ultrasonic vibration); C-zinc phosphating coating (adding hydroxylamine sulphate); D-zinc phosphating coating (introducing constant-intensity ultrasonic vibration); E-zinc phosphating coating (synergistic effect of hydroxylamine sulphate and constant-intensity ultrasonic vibration)

The reason is that the zinc phosphating coating prepared without hydroxylamine sulphate is incomplete and has a limited protective effect on 20# steel. The polarization curves of zinc phosphating coatings prepared by adding hydroxylamine sulphate and introducing constant-intensity ultrasonic vibration deviate to the upper left compared with the polarization curve of 20# steel, indicating that both kinds of zinc phosphating coatings can enhance the protective effect of 20# steel, and both can inhibit the corrosion of 20# steel to a certain extent. The polarization curve of the zinc phosphating coating prepared by synergistic effect of hydroxylamine sulphate and constant-intensity ultrasonic vibration has a more offset polarization curve than that of 20# steel, indicating that the zinc phosphating coating can better inhibit corrosion of 20# steel.

As can be seen from Table 1, compared with 20# steel, the corrosion potential of different zinc phosphatizing coatings prepared by adding hydroxylamine sulphate, introducing constant-intensity ultrasonic vibration and synergistic effect of hydroxylamine sulphate and constant-intensity ultrasonic vibration respectively has varying degrees of positive shift, and the corrosion current density has different degrees of decrease. Among them, the phosphating coating prepared by synergistic effect of

hydroxylamine sulphate and constant-intensity ultrasonic vibration has the best corrosion resistance with the lowest corrosion current density of 1.56×10^{-6} A/cm^2 which is better than some zinc phosphating coatings reported [28-29].

Table 1. Polarization curves fitting results

Different samples	Corrosion potential / V	Corrosion current density/ (A·cm^2)
20# steel	-0.510	6.071×10^{-5}
zinc phosphating coating (without hydroxylamine sulphate and constant-intensity ultrasonic vibration)	-0.506	5.184×10^{-5}
zinc phosphating coating (adding hydroxylamine sulphate)	-0.485	8.242×10^{-6}
zinc phosphating coating (introducing constant-intensity ultrasonic vibration)	-0.476	7.050×10^{-6}
zinc phosphating coating (synergistic effect of hydroxylamine sulphate and constant-intensity ultrasonic vibration)	-0.441	1.563×10^{-6}

3.4.2 Electrochemical impedance spectroscopy analysis

Figure 6 shows the electrochemical impedance spectroscopy of 20# steel and different zinc phosphating coatings immersed in 3.5% sodium chloride solution for 96 h, Table 2 shows the analytical results of electrochemical impedance spectroscopy. The charge transfer resistance and coating resistance are proved that can be used to evaluate the corrosion resistance of materials [30-31]. As can be seen from Figure 6, there is little difference between the arc radius of zinc phosphating coating prepared without hydroxylamine sulphate and that of 20# steel, which also proves that the phosphating coating cannot effectively inhibit the corrosion of 20# steel. The capacitive resistance arc radius of the zinc phosphating coating prepared by adding hydroxylamine sulphate or introducing constant-intensity ultrasonic vibration both increases, but is smaller than that of the zinc phosphating coating prepared by synergistic effect of hydroxylamine sulphate and constant-intensity ultrasonic vibration. Compared with 20# steel (charge transfer resistance and coating resistance are 1830 Ω·cm^2 and 572 Ω·cm^2, respectively), the charge transfer resistance of the zinc phosphating coating prepared by adding hydroxylamine sulphate or introducing constant-intensity ultrasonic vibration is about 3240 Ω·cm^2 and 3820 Ω·cm^2, respectively. Furthermore, the coating resistance of the zinc phosphating coating prepared by adding hydroxylamine sulphate or introducing constant-intensity ultrasonic vibration is about 1830 Ω·cm^2 and 1232 Ω·cm^2, respectively. The charge transfer resistance and coating resistance of the zinc phosphating coating prepared by synergistic effect of hydroxylamine

sulphate and constant-intensity ultrasonic vibration are increased to 4370 Ω·cm^2 and 1440 Ω·cm^2, respectively. The increase of capacitive resistance arc radius, charge transfer resistance and coating resistance means that the corrosion resistance of zinc phosphating coating is improved [32-33].

Adding hydroxylamine sulphate or introducing constant-intensity ultrasonic vibration can promote the phosphating reaction and form a complete and relatively dense zinc phosphating coating to block corrosion medium and reduce the corrosion tendency of 20# steel. However, the synergistic effect of hydroxylamine sulphate and constant-intensity ultrasonic vibration can not only reduce the addition amount of hydroxylamine sulphate, but also promote more compact zinc phosphating coating with the best corrosion resistance, so as to better inhibit the corrosion of 20# steel.

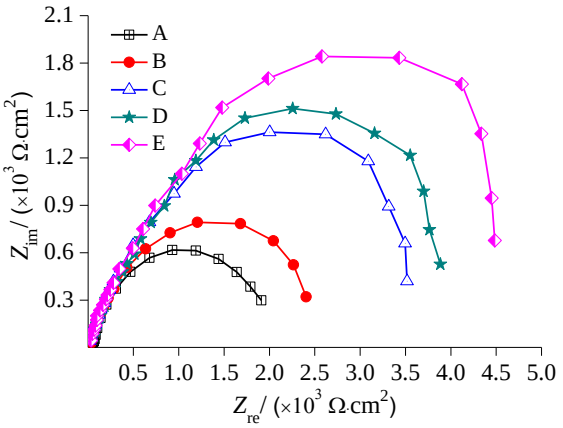

Figure 6. Electrochemical impedance spectroscopy of 20# steel and different zinc phosphating coatings immersed in 3.5% sodium chloride solution for 96 h: A-20# steel; B-zinc phosphating coating (without hydroxylamine sulphate and constant-intensity ultrasonic vibration); C-zinc phosphating coating (adding hydroxylamine sulphate); D-zinc phosphating coating (introducing constant-intensity ultrasonic vibration); E-zinc phosphating coating (synergistic effect of hydroxylamine sulphate and constant-intensity ultrasonic vibration)

Table 2. Analytical results of electrochemical impedance spectroscopy

Different samples	Charge transfer resistance/ (Ω·cm^2)	Coating resistance/ (Ω·cm^2)
20# steel	1830	572
zinc phosphating coating (without hydroxylamine sulphate and constant-intensity ultrasonic vibration)	2265	730
zinc phosphating coating (adding hydroxylamine sulphate)	3240	1080
zinc phosphating coating (introducing constant-intensity ultrasonic vibration)	3820	1232
zinc phosphating coating (synergistic effect of hydroxylamine sulphate and constant-intensity ultrasonic vibration)	4370	1440

3.4.3 Corrosion weight loss and corrosion morphology analysis

Figure 7 shows the corrosion weight loss of 20# steel and different zinc phosphating coatings immersed in 3.5% sodium chloride solution for 96 h. It can be seen from Figure 7 that the corrosion weight loss of the zinc phosphating coating prepared without hydroxylamine sulphate is not much different from that of 20# steel, which is owing to the limited protective effect of the phosphating coating on 20# steel. The corrosion weight loss of the zinc phosphating coatings prepared by adding hydroxylamine sulphate or introducing constant-intensity ultrasonic vibration is both reduced to a certain extent. The corrosion weight loss of the zinc phosphating coating prepared by synergistic effect of hydroxylamine sulphate and constant-intensity ultrasonic vibration has been reduced even further to 2.7 g/m^2, confirming that it has the best corrosion resistance and can better inhibit the corrosion of 20# steel.

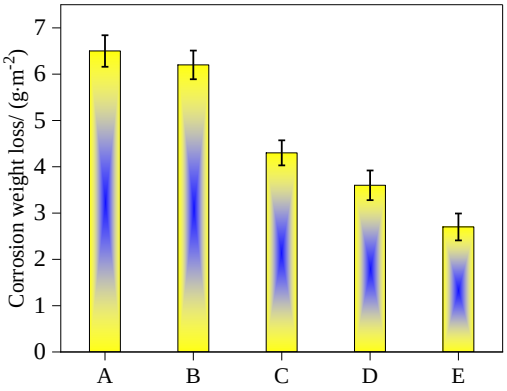

Figure 7. Corrosion weight loss of 20# steel and different zinc phosphating coatings immersed in 3.5% sodium chloride solution for 96 h: A-20# steel; B-zinc phosphating coating (without hydroxylamine sulphate and constant-intensity ultrasonic vibration); C-zinc phosphating coating (adding hydroxylamine sulphate); D-zinc phosphating coating (introducing constant-intensity ultrasonic vibration); E-zinc phosphating coating (synergistic effect of hydroxylamine sulphate and constant-intensity ultrasonic vibration)

Figure 8 shows the corrosion morphology of 20# steel and different zinc phosphating coatings immersed in 3.5% sodium chloride solution for 96 h. As can be seen from Figure 8(a), 20# steel is severely corroded and its surface is cracked with deep cracks.

Loose corrosion products accumulated on the surface of 20# steel will guide chloride ions and other corrosive media to penetrate, so as to further aggravate the corrosion of 20# steel. The corrosion mechanism of steel has been widely reported in the literature [34-35]. It can be seen from Figure 8(b) that the zinc phosphating coating prepared without hydroxylamine sulphate also has serious corrosion, which further confirms poor corrosion resistance and limited protective effect on 20# steel. As can be seen from Figure 8(c) and Figure 8(d), the corrosion degree of the zinc phosphating coating prepared by adding hydroxylamine sulphate or introducing constant-intensity ultrasonic vibration is

significantly reduced compared with the zinc phosphating coating prepared without hydroxylamine sulphate.

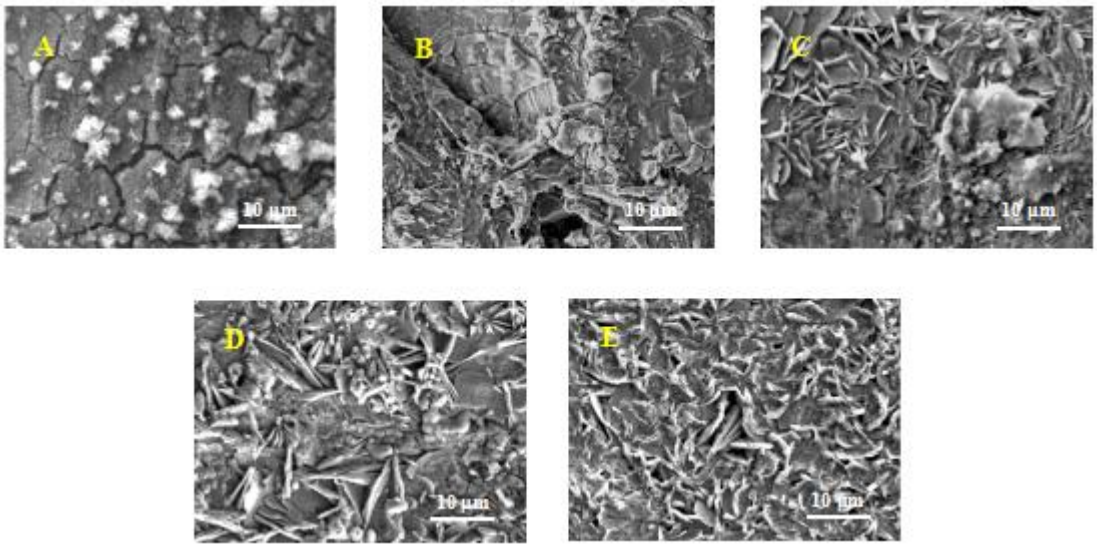

Figure 8. Surface morphology of 20# steel and different zinc phosphating coatings immersed in 3.5% sodium chloride solution for 96 h: A-20# steel; B-zinc phosphating coating (without hydroxylamine sulphate and constant-intensity ultrasonic vibration); C-zinc phosphating coating (adding hydroxylamine sulphate); D-zinc phosphating coating (introducing constant-intensity ultrasonic vibration); E-zinc phosphating coating (synergistic effect of hydroxylamine sulphate and constant-intensity ultrasonic vibration)

According to Figure 8(e), the surface of the zinc phosphating coating prepared by synergistic effect of hydroxylamine sulphate and constant-intensity ultrasonic vibration is still smooth and compact after corrosion, with few defects, and the corrosion degree is the lightest.

4. CONCLUSIONS

(1) Adding hydroxylamine sulphate or introducting constant-intensity ultrasonic vibration can promote phosphating reaction and contribute to the formation of a complete and relatively dense zinc phosphating coating, which is primarily composed of $Zn_3(PO_4)_2{\cdot}4H_2O$ and $Zn_2Fe(PO_4)_2{\cdot}4H_2O$ phases. Compared with the zinc phosphating coating prepared without hydroxylamine sulphate, the corrosion resistance of the zinc phosphating coating prepared by adding hydroxylamine sulphate or introducting constant-intensity ultrasonic vibration is improved and the protective effect on 20# steel is enhanced.

(2) The synergistic effect of hydroxylamine sulphate and constant-intensity ultrasonic vibration can prepare a zinc phosphating coating with better compactness under the condition of reducing the amount of hydroxylamine sulphate added. The zinc phosphating coating prepared by synergistic effect of hydroxylamine sulphate and constant-intensity ultrasonic vibration has a corrosion current density

of only 1.56×10^{-6} A/cm^2 and corrosion weight loss of only 2.7 g/m^2, which can better inhibit the corrosion of 20# steel.

References

1. L. Kouisni, M. Azzi, M. Zertoubi, F. Dalard and S. Maximovitch, *Surf. Coat. Technol.*, 185 (2004) 58.
2. A. H. Riyas, C. V. Geethanjali, S. Arathy, A. Anil and S. M. A. Shibli, *Appl. Surf. Sci.*, 593 (2022) 153370.
3. Y. D. Yu, G. Y. Wei, J. W. Lou, H. L. Ge, L. X. Sun and L. Z. Zhu, *Surf. Eng.*, 29 (2013) 234.
4. J. Rodrigues, S. O. Pereira, J. Zanoni, B. P. Falcao, N. F. Santos, J. P. Moura, M. R. Soares, L. Rino, F. M. Costa and T. Monteiro, *Mater. Today Chem.*, 23 (2022) 100629.
5. J. Liu, B. Zhang, W. H. Qi, Y. G. Deng and R. D. K. Misra, *J. Mater. Res. Technol.*, 9 (2020) 5912.
6. D. W. Zhao, C. Liu, K. Q. Zuo, P. Su, L. B. Li, G. Y. Xiao and L. Cheng, *Chem. Eng. J.*, 408 (2021) 127362.
7. F. Fang, J. H. Jiang, S. Y. Tan, A. B. Ma and J. Q. Jiang, *Surf. Coat. Technol.*, 204 (2010) 2381.
8. R. X. Li, Q. M. Yu, C. P. Yang, H. Chen, G. X. Xie and J. Y. Guo, *J. Cleaner Prod.*, 18 (2010) 1040.
9. M. Abbasi and M. M. Attar, *J. Coat. Technol. Res.*, 14 (2017) 1435.
10. H. Y. Du, X. J. Ren, D. Pan, Y. L. An, Y. H. Wei, X. D. Liu, L. F. Hou, B. S. Liu, M. M. Liu and Z. H. Guo, *Adv. Compos. Hybrid Mater.*, 4 (2021) 401.
11. T. Distler, *IST Int. Surf. Technol.*, 9 (2016) 34.
12. I. D. Kosobudskii, Y. V. Seryanov and N. M. Trepak, *Inorg. Mater.*, 36 (2000) 580.
13. Y. D. Yu, Z. L. Song, H. L. Ge and G. Y. Wei, *Prog. Nat. Sci.: Mater. Int.*, 24 (2014) 232.
14. C. M. Gui, C. G. Yao, J. J. Huang and G. S. Yang, *J. Mater. Sci.: Mater. Electron.*, 29 (2018) 5561.
15. X. X. Sun, M. Y. Liu, J. C. Song and Y. S. Xu, *Geothermics*, 86 (2020) 101807.
16. K. He, G. Y. Xiao, W. H. Xu, R. F. Zhu and Y. P. Lu, *Ultrason. Sonochem.*, 21 (2014) 499.
17. H. J. Zhang, L. H. Li, N. Chen, H. J. Ben, G. M. Zhan, H. W. Sun, Q. Li, J. Sun and L. Z. Zhang, *Appl. Catal., B*, 312 (2022) 121410.
18. M. G. Prodanchuk, A. M. Tsatsakis, G. M. Proanchuk and A. K. Tsakalof, *Food Chem. Toxicol.*, 61 (2013) 227.
19. V. K. Bajpai, H. Pandey, T. Singh and P. Dixit, *Mater. Lett.*, 316 (2022) 132033.
20. A. X. Li, Z. W. Zhu, Y. P. Liu and T. Y. Li, *Ultrason. Sonochem.*, 82 (2022) 105894.
21. Y. G. Bu, X. L. Liu, J. A. Turner, Y. F. Song and X. B. Li, *NDT & E Int.*, 117 (2021) 102369.
22. M. Norouzian, S. Islam and J. A. Turner, *Ultrasonics*, 102 (2020) 106032.
23. C. Guo, J. Liu, X. H. Li and S. Q. Yang, *Ultrason. Sonochem.*, 79 (2021) 105782.
24. C. Peng, C. Y. Zhang, Q. F. Li, S. L. Zhang, Y. Su, H. R. Lin and J. H. Fu, *Adv. Powder Technol.*, 32 (2021) 4391.
25. L. Z. Ye, X. J. Zhu and Y. Liu, *Ultrason. Sonochem.*, 59 (2019) 104744.
26. T. Baloyi, N. Maledi and A. Andrews, *Mater. Chem. Phys.*, 283 (2022) 126009.
27. N. V. Phuong, K. Lee, D. Chang, M. Kim, S. Lee and S. Moon, *Met. Mater. Int.*, 19 (2013) 273.
28. W. Zai, X. R. Zhang, Y. C. Su, H. C. Man, G. Y. Li and J. S. Lian, *Surf. Coat. Technol.*, 397 (2020) 125919.
29. N. V. Phuong and S. Moon, *Mater. Lett.*, 122 (2014) 341.
30. P. Mishra, D. Yavas, A. F. Bastawros and K. R. Hebert, *Electrochim. Acta*, 346 (2020) 136232.
31. A. M. KamalanKirubaharan, A. Anderson, K. G. Saravanan, M. Rajasekaramoorthy and R.

Balachandar, *Mater. Today:. Proc.*, 33 (2020) 902.
32. A. Thoriya, T. Vora and P. Nyanzi, *Mater. Today:. Proc.*, 56 (2022) 2334.
33. P. Slepski, M. Szocinski, G. Lentka and K. Darowicki, *Measurement*, 173 (2021) 108667.
34. D. W. Niu, C. X. Zhang, X. D. Sui, X. L. Lu, X. Zhang, C. Wang, J. Y. Hao and Z. Q. Shi, *Tribol. Int.*, 173 (2022) 107638.
35. L. Nyrkova, S. Melnichuk, S. Osadchuk, P. Lisovyi and S. Prokopchuk, *Mater. Today:. Proc.*, 50 (2022) 470.